HIERARCHICAL SIMULATION OF THE SPATIOTEMPORAL EVOLUTION OF HETEROGENEOUS BIOFILMS AND THEIR IMPACT ON THE FLOW PATTERN AND MASS TRANSPORT IN 3-D POROUS MEDIA

G.E. KAPELLOS, T.S. ALEXIOU, S. PAVLOU, A.C. PAYATAKES

Department of Chemical Engineering, University of Patras, and FORTH/Institute of Chemical Engineering and High Temperature Chemical Processes, GR-26504, Greece

ABSTRACT

A computer-aided simulator has been developed for the prediction of the pattern of evolution and the rate of growth of heterogeneous biofilms within the pore space of 3-D virtual porous media (core-scale). The biofilm itself is considered as a heterogeneous porous material that exhibits a hierarchy of length scales. A recently developed theoretical model, which takes into account fundamental geometric and physicochemical properties of the biofilm at the cell- and molecular-scales, is used to calculate the values of the *local* hydraulic permeability and diffusion coefficient within it. Modified Navier-Stokes-Brinkman equations are solved numerically to determine the velocity and pressure fields within the pore space, which is occupied partly by free fluid and partly by biofilms. Under the action of large fluid shear stresses biofilm fragments become detached and re-enter into the free fluid stream. A Lagrangian-type simulation is used to determine the trajectories of the detached fragments until they exit from the system or re-attach to downstream grain or biofilm surfaces. Furthermore, the spatiotemporal distributions of nutrients and soluble cellular products are determined from the numerical solution of the governing convection-diffusion-reaction equations. The simulator incorporates growth and apoptosis kinetics for the bacterial cells and production and lysis kinetics for the extracellular polymeric substances that compose the biofilm. Growth-induced deformation of the biofilms is implemented by using a cellular automaton approach. Transient changes in the pore geometry caused by biofilm proliferation intensify the formation of preferential flowpaths within the porous medium. The decrease of permeability caused by clogging of the porous medium is calculated and is found to be in qualitative agreement with published experimental results.

1. INTRODUCTION

Many bacteria are able to attach, grow and eventually form biofilms on solid surfaces if favorable local environmental conditions persist. The term biofilm is used to describe a microbial consortium immobilized on a solid surface and embedded in a fibrous, highly hydrated matrix of extracellular polymeric substances (EPS) with complex three-dimensional architecture [*Costerton et al.*, 1994]. Porous media are exquisite *hosts* for biofilm-forming bacteria because of their high specific surface [*Rittmann*, 1993]. The process of biofilm growth in porous media is of key importance in a variety of natural phenomena and technological applications, such as natural attenuation of organic contaminants by indigenous

bacteria in soil and aquifers, microbially enhanced oil recovery from subsurface reservoirs, water and wastewater treatment in fixed and fluidized biofilters, etc.

The analysis of such processes is not trivial because the structure of the physical system under consideration exhibits a *hierarchy of characteristic length scales* that spans several orders of magnitude and, further, there exists an intricate interplay of hydrodynamic, physicochemical and biological processes at several different *characteristic time scales*. In addition, each structural level might be heterogeneous with respect to geometrical and topological characteristics (e.g. pore and grain size, shape and connectivity), physical properties (e.g. fluid density and viscosity), chemical composition (e.g. mineralogy of the solid matrix), as well as biological composition and activity (e.g. number and physiological state of bacterial cells). Mathematical models and simulators are valuable tools for the elucidation of the underlying mechanisms and the prediction of the behavior of these complex processes. Up to date, significant work has been devoted in the development of models for this process on a single length scale (e.g., field or pore scale), neglecting what happens at smaller and/or larger length scales. However, the process under consideration is inherently multiscale, meaning that the different length scales interact strongly to produce the observed behavior. For example, the macroscale properties of the porous medium (permeability, dispersion coefficient, etc.) depend strongly on the detailed spatial distribution and the corresponding properties of the biofilms at the core-scale (a few cm).

We have developed a hierarchical simulator (HiBioSim-PM) that predicts: i) the structural and biological heterogeneity at the biofilm scale, and ii) the pattern of evolution and the rate of growth of heterogeneous biofilms within the pore space of porous media (core scale) [*Kapellos et al.*, 2005, 2006]. At the core-scale, we combine a deterministic, continuum-based approach for the description of fluid flow and solute transport and a stochastic, individual-based approach for the description of biofilm growth. The rationale for the development of this *hybrid* approach is the disparity in characteristic lengths between chemical species and biofilms. The local values of the hydraulic permeability and the diffusion coefficient within the biofilm are calculated using a recently developed "effective-medium" model, which takes into account fundamental geometric and physicochemical properties at the cell- and macromolecular- length scales. In this work, we investigate the impact of biofilm growth on the flow pattern and the mass transport of chemical species in a 3D packing of spherical grains.

2. DESCRIPTION OF THE HIERARCHICAL SIMULATOR

Here we provide a brief description of the hierarchical simulator, whereas a more detailed one is given by *Kapellos et al.* [2006]. The simulation proceeds as follows.

2.1 Step 1: Generation of the pore structure.

The overall porosity as well as the number and the radius distribution of the grains are prescribed and a collective rearrangement algorithm is used to construct a 3-D virtual random packing of spherical grains.

2.2 Step 2: Inoculation of the porous medium.

The initial flow field within the pore space is determined as described in Step 6. Then, a single microbial cell at a time is inserted randomly at the inflow boundary of the virtual

porous medium and moves along the streamlines (see Step 7) until it is captured at a grain surface. This procedure is repeated until the number of initially attached bacteria equals a prescribed value.

2.3 Step 3: Biofilm growth.

With regard to the biological processes, biofilm is treated as a population of interacting unit biomass cells (UBCs), each of which contains bacterial cells, hydrated EPS and water. The UBCs are cubic in shape with dimensions on the order of several bacterial cell diameters. A state vector is assigned to each UBC. This contains the volume fractions of the bacterial cells, hydrated EPS, and water, as well as the number, the mass, and the physiological status (active, dormant or apoptotic) of the bacterial cells. The bacterial cells within the same UBC are considered as *tied to a common fate*, meaning that they grow, proliferate and die all together. The active bacterial cells consume the carbon source and electron acceptor and synthesize new cellular mass with rate proportional to their mass. Part of the cellular mass is used for maintenance purposes (endogenous metabolism). Simultaneously, they synthesize and secrete EPS within their UBC with rate proportional to their growth rate. Part of the EPS matrix lyses (say due to enzymatic or hydrolytic action) with rate proportional to its mass. Based on these assumptions the mass balances for bacterial cells and EPS within a UBC are

$$\frac{dX_\kappa}{dt} = \mu_{\kappa,g} X_\kappa - \mu_{\kappa,m} X_\kappa \tag{1}$$

$$\frac{dX_\pi}{dt} = Y_{\pi/\kappa} \mu_{\kappa,g} X_\kappa - k_{lys} X_\pi \tag{2}$$

where X_κ, X_π is the mass of cells, EPS over the volume of UBC, and $\mu_{\kappa,g}$, $\mu_{\kappa,m}$, $Y_{\pi/\kappa}$, k_{lys} are kinetic parameters, which might be defined as functions of the local environmental conditions (concentrations of pollutants, electron acceptor, mechanical stresses, temperature, pH, etc.). If the specific growth rate is greater than a critical value, $\mu_{\kappa,g,crit}$, the active bacterial cells continuously increase their mass until it exceeds a prescribed upper threshold value, $m^+_{\kappa,crit}$. Then they divide into two equal daughter cells (the number of cells within the UBC doubles and the mass of each cell halves). If the specific growth rate gets lower than the critical value, the cells enter the dormancy state during which the metabolic activity is halted and only consumption of cellular mass for maintenance purposes takes place. Dormant cells may be activated once again if the specific growth rate is restored to a value greater than the critical. During dormancy, cellular mass decreases continuously until a prescribed lower threshold value, $m^-_{\kappa,crit}$, is reached. Then the cells enter the apoptosis state (programmed cell death), which is irreversible and lysis of the cells occurs with probability

$$p_{ap}(\tau_{ap}) = 1 - \exp(-k_{ap}\tau_{ap}) \tag{3}$$

where τ_{ap} is the time interval since the cells became apoptotic and k_{ap} is the apoptosis rate constant.

2.4 Step 4: Biofilm Proliferation.

To implement growth-induced deformation of the biofilm a cellular-automaton approach is taken here. First, the entire pore space is discretized in UBCs. Thus, apart from the regular UBCs that contain biomass (cells plus EPS), there are also empty-UBCs that reside in clear

fluid regions. If the mass of bacterial cells or EPS within a UBC exceeds a corresponding, prescribed maximum allowable value then *biomass percolates* from the overgrown UBC towards the nearest empty-UBC along the *path of least mechanical resistance*. In particular, a random walk procedure is used to generate a large number of paths that connect the overgrown UBC and the nearest empty-UBC, without passing over solid obstacles, and the shortest of them is chosen. If there are more than one paths with the same minimum length, then the path that passes through the lowest overall biomass is chosen. Afterwards, the overgrown UBC displaces its adjacent UBC (defined by the path) and thus generates a temporarily empty-UBC in which it puts half of its biomass, while it retains the other half. The displaced UBC in turn displaces its adjacent UBC and takes its position. This sequence of interactions continues until the end position of the path.

2.5 Step 5: Calculation of the local hydraulic permeability and diffusion coefficients within the biofilm.

A recently developed "effective-medium" model is used to calculate the local hydraulic permeability and diffusion coefficient within the biofilm [more information is given by *Kapellos et al.*, (2004) and the complete formulation will appear elsewhere]. The effective-medium is a conceptual homogeneous medium that is assumed to have the same macroscopic properties with the (microscopically) inhomogeneous medium [*Choy*, 1999]. A unit cell model embedded in an effective-medium to represent the structure of a randomly inhomogeneous volume of biofilm (Figure 4). The simplified unit cell model represents the structure in the vicinity of a single bacterial cell. Specifically, a composite sphere, comprising a rigid spherical core surrounded by a concentric spherical porous shell, represents a single bacterial cell surrounded by hydrated, fibrous EPS matrix. The composite sphere is surrounded by a concentric spherical fluid envelope and together are embedded in an exterior effective porous medium. The fluid envelope: a) represents the volume between neighboring bacterial cells that is occupied by water and b) constitutes a first order approximation for the fluctuation of the local mean density that is observed in the real system. The exterior effective medium represents the neighboring bacterial cells and the EPS in which they are enmeshed. The creeping flow and passive diffusion problems have been solved analytically in the geometric unit cell configuration and closed-form expressions have been obtained for the calculation of the hydraulic permeability and diffusion coefficient of a dissolved substance (here organic pollutants and electron acceptor). These expressions are functions of geometrical (volume fractions of cells, EPS and water, average diameter of cells, average diameter of EPS fibers, internal porosity of the EPS, average thickness of the cell membrane) and physicochemical (dynamic viscosity of the fluid, diffusivity of the substance in water and cell membrane, partition coefficient of the substance in the fluid-membrane interface) properties.

2.6 Step 6: Determination of the flow field.

Single-phase flow of an incompressible Newtonian fluid (say a dilute aqueous solution) is considered within the pore space of the granular porous medium, which is occupied partly by fluid and partly by porous biofilms. Within the fluid regions, the Navier-Stokes equations and the continuity equation result from the formulation of the momentum and mass balance, respectively. Within the porous biofilm, Brinkman's extension of Darcy's law is considered as an appropriate equation to describe the flow along with the conservation of total mass. At

this point, the analysis is substantially simplified if the pore space is treated as a single composite medium with spatially varying properties. The final equations are

$$\nabla \cdot \mathbf{v} = 0 \tag{4}$$

$$\rho\left[\frac{\partial \mathbf{v}}{\partial t} + \alpha_c \nabla \cdot (\mathbf{v}\mathbf{v}/\varepsilon)\right] = -\varepsilon \nabla P + \mu \nabla^2 \mathbf{v} - \frac{\varepsilon(1-\alpha_c)}{k}\mathbf{v} \tag{5}$$

where $\mathbf{v}$ is the local superficial velocity of the fluid (averaged with respect to the total volume), P is the intrinsic pressure of the fluid modified properly to account for the gravity potential (averaged with respect to the volume of fluid), μ is the fluid viscosity, ρ is the fluid density, ε is the local volume fraction of fluid, k is the local hydraulic permeability (defined only within the regions of porous biofilms) and α_c is a computational parameter that equals unity within regions of fluid and zero within regions of biofilms). The final term at the right hand of eq.-(5) is used to incorporate the fluid-solid interactions that prevail in regions of porous biofilms. This approach is usually referred to as single-domain approach. Equations (4)-(5) are solved numerically using a staggered grid for the spatial discretization, central finite differences for the viscous and pressure terms and a higher-order upwinding scheme for the inertial terms.

2.7 Step 7: Detachment, motion and reattachment of biofilm fragments.

If a UBC is adjacent to clear fluid then the average shear stress acting on the surfaces exposed to fluid is calculated and if it exceeds a designated critical stress value the UBC is considered to loose the cohesiveness with adjacent UBCs or solid surfaces. Then the UBC begins to move along the fluid streamlines as if a fluid element (in a first approximation the effects of gravity and drag forces are neglected based on the facts that biofilm is highly porous and its density is very close to that of the aqueous solution). The trajectory of the UBC within the pore space is calculated from the numerical integration of

$$\frac{d\mathbf{r}_p}{dt} = \mathbf{v} \tag{6}$$

where $\mathbf{r}_p$ is the position of the mass center of the UBC at time t. The UBC stops moving if it gets over the outflow boundary of the porous medium or if it becomes reattached to grain or biofilm surface, which is exposed to shear stress lower than the critical value. If at least one UBC has been detached, the simulator is directed to Step 6 again.

2.8 Step 8: Determination of concentration profiles.

The fate of the ith-dissolved substance (organic pollutant or electron acceptor) is determined from the convection-diffusion-reaction equation

$$\frac{\partial}{\partial t}\left[\sum_j \gamma_{ij} C_i\right] + \nabla \cdot \left(\mathbf{v} C_i\right) = \nabla \cdot \left[D_{i,eff} \nabla C_i\right] + R_i \tag{7}$$

where C_i, is the concentration, $D_{i,eff}$ is the local effective diffusivity and R_i is the local reaction rate (usually assumed to be proportional to the local growth rate of bacterial cells) of the ith-dissolved substance. Further, γ_{ij} is the partition coefficient of the ith-substance in the jth-phase (fluid, bacterial cells or EPS). This formulation takes into account the potential reversible adsorption of chemical species in the EPS matrix and equilibrium partition in the bacterial cells. Equation (7) is solved using a fractional step method, in which the solution procedure is split up into independent steps corresponding to the convection, diffusion and

reaction processes and each step is solved independently. An explicit in time, higher-order upwinding scheme is used for the convective terms, implicit central differencing is used for the diffusive terms and the explicit fourth order Runge-Kutta method is used for the reaction terms. The simulator is directed to Step 3.

3. SAMPLE SIMULATION RESULTS

Here, we present sample simulation results of biofilm growth in a periodic, regular 3D packing of spherical grains. The values of the physicochemical, biological and operational parameters used in this simulation are the same with those used by *Kapellos et al.* [2006, Table 1]. Figure 1 shows snapshots of the spatial distribution of biofilms (green colour) and the corresponding flow patterns within the porous medium at three different time instants. Note that the streamlines are equidistant and the starting points are the same in all three cases (1d-f). Figure 2 shows the temporal evolution of the accumulated biomass in the pore space, as well as of the amount of the convected-out biomass. The transient decrease of the overall porosity and the permeability of the porous medium are shown in Figure 3. The predicted behavior is in qualitative agreement with the experimental results of *Cunningham et al.* [1991]. Figure 4 shows the breakthrough curve of an inert solute at two different time instants. We observe that the presence of the biofilms decreases the time required for solute breakthrough. This trend is in qualitative agreement with the experimental results of *Sharp et al.*, [1999]. In conclusion, the growth of biofilms in porous media is a strongly dynamic process and affects significantly fluid flow and solute transport within the porous medium (at least, for the conditions used in this simulation).

REFERENCES

Choy, T.C. (1999), *Effective medium theory. Principles and applications*, Oxford University Press, Great Britain.

Cunningham, A.B., W.G. Characklis, F. Abedeen, and D. Crawford (1991), Influence of biofilm accumulation on porous media hydrodynamics, *Environ. Sci. Technol.*, *25*, 1305.

Costerton, J.W., Z. Lewandowski, D. DeBeer, D. Caldwell, D. Korber, and G. James (1994), Biofilms, the customized microniche, *J Bacteriol*, *176*, 2137.

Kapellos, G.E., T.S. Alexiou, S. Pavlou, and A.C. Payatakes (2004), Hierarchical modeling approach for the prediction of effective hydraulic permeability and diffusion coefficient in biofilms, in *Proceedings of the International Conference Biofilms 2004: Biofilm Structure and Activity*, Las Vegas, NV, USA, p.255-260.

Kapellos, G.E., T.S. Alexiou, S. Pavlou, and A.C. Payatakes (2005), Hierarchical simulation of biofilm dynamics in porous media during the biodegradation of organic pollutants, paper presented at the 3rd European Conference on Bioremediation, Chania, Greece, 4-7 July.

Kapellos, G.E., T.S. Alexiou, and A.C. Payatakes (2006), Hierarchical simulator of biofilm growth and dynamics in granular porous materials, *Adv Water Resour* (accepted).

Rittmann, B.E. (1993), The significance of biofilms in porous media, *Water Resour Res, 29(7)*, 2195.

Sharp, R.R., A.B. Cunningham, J. Komlos, and J. Billmayer (1999), Observation of thick biofilm accumulation and structure in porous media and corresponding hydrodynamic and mass transfer effects, *Water Sci Technol*, *39(7)*, 195.

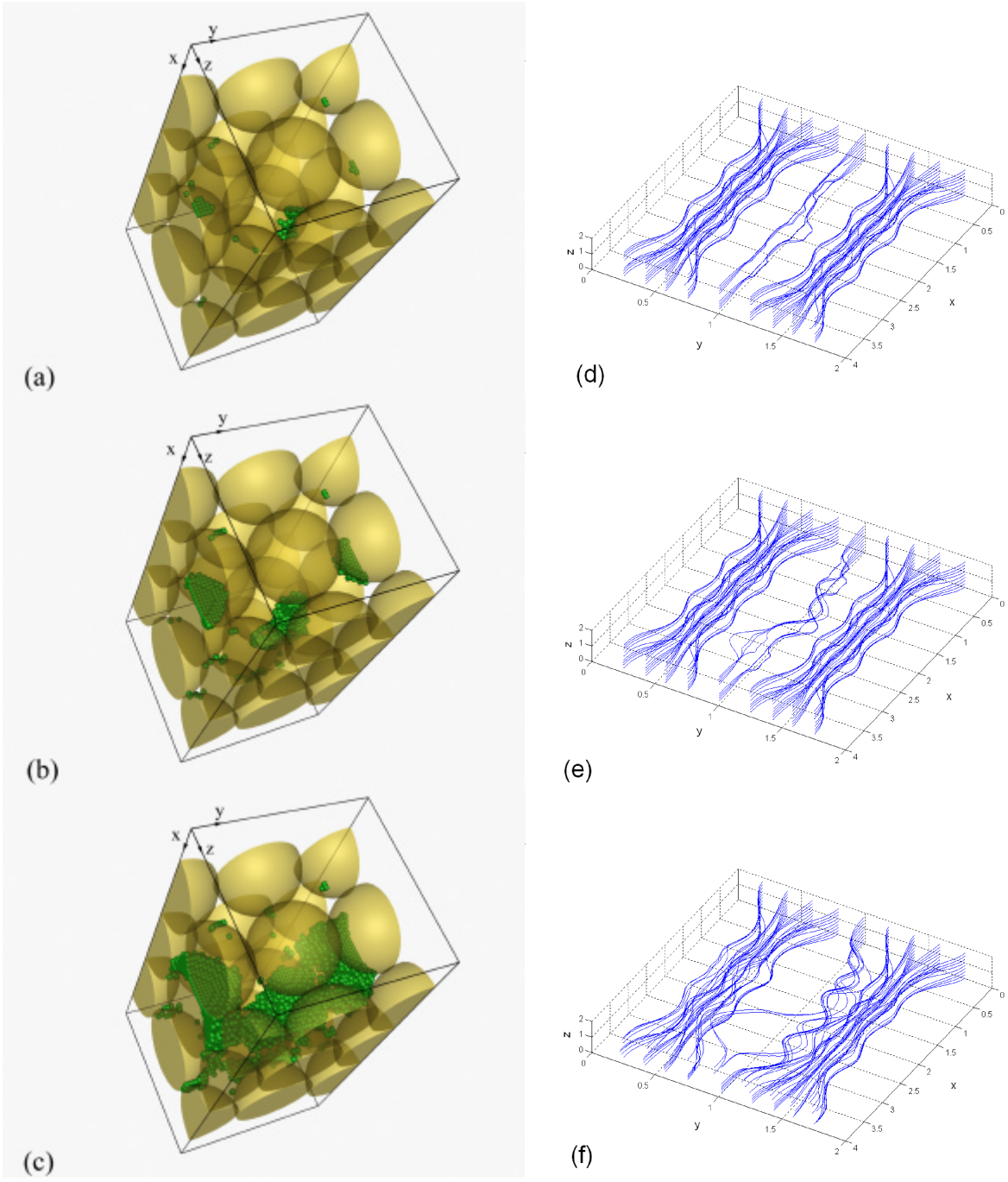

FIGURE 1. Snapshots of the spatial distribution of the biofilms (a-c) and the flow pattern (d-f) in the 3D packing at three different time instants: (a) τ=20, (b) τ=30, (c) τ=40, (d) τ=20, (e) τ=30, (f) τ=40, where $\tau = \mu_{max} t$, and μ_{max} is the maximum specific growth rate of microbial cells. The biofilms are in green colour. The grains are semi-transparent for better visualization of the biofilms. The streamlines in d-f are equidistant and start from the same points in all three cases.

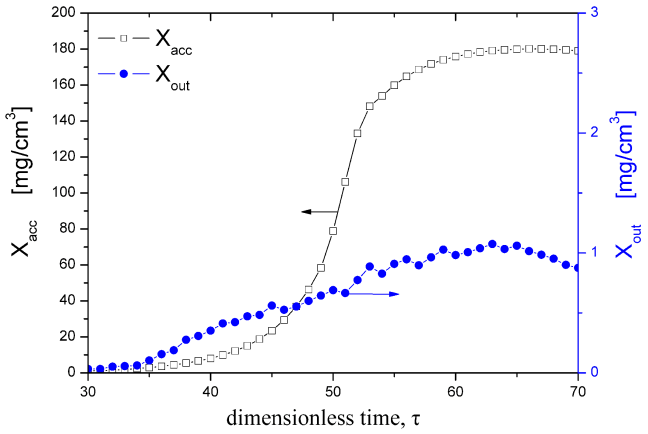

FIGURE 2. Temporal evolution of accumulated biomass in the porous medium per unit of initial pore volume, X_{acc}, and convected-out biomass per unit of initial pore volume, X_{out}.

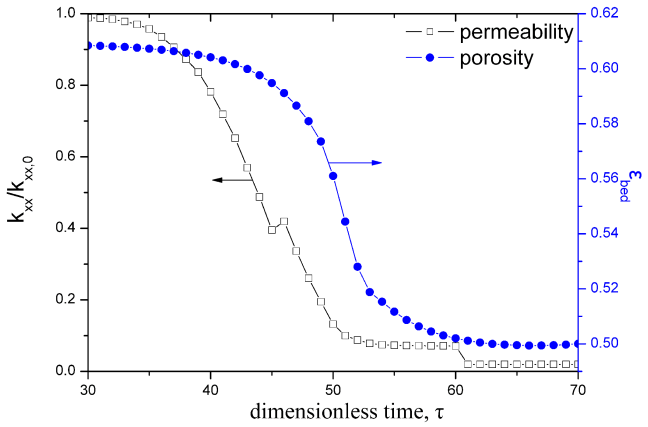

FIGURE 3. Temporal evolution of the porosity (accounting for the extracellular water in the biofilms) and the permeability of the porous medium ($k_{xx,0}$ = permeability of the clean bed).

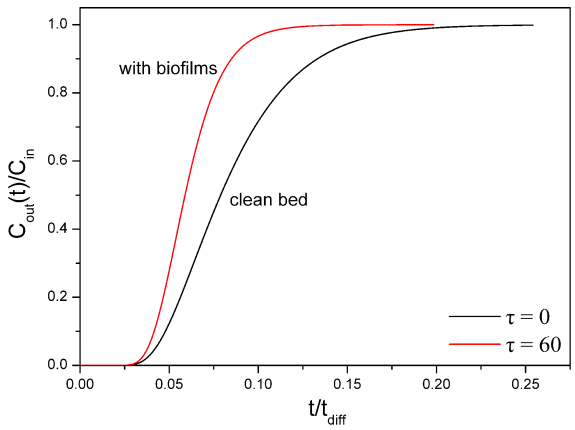

FIGURE 4. Breakthrough curves for an inert solute for two different configurations of the pore space (t_{diff}=characteristic time for diffusion of the solute) .